Genesis and Exhumation Dynamics of Eclogites in the Kokchetav Massif near Mount Sulu-Tyube, Kazakhstan

Article *in* Geochemistry International · October 1998

Alexei L. Perchuk
Lomonosov Moscow State University

Geochemistry International, Vol. 36, No. 10, 1998, pp. 877–885. Translated from Geokhimiya, No. 10, 1998, pp. 979–988.

Genesis and Exhumation Dynamics of Eclogites in the Kokchetav Massif near Mount Sulu-Tyube, Kazakhstan

A. L. Perchuk*, V. O. Yapaskurt, and S. K. Podlesskii*****

* *Institute of the Geology of Ore Deposits, Petrography, Mineralogy, and Geochemistry (IGEM), Russian Academy of Sciences, Staromonetnyi per. 35, Moscow, 109017 Russia*

** *Faculty of Geology, Moscow State University, Vorob'evy gory, Moscow, 119899 Russia*

*** *Faculty of Mechanics and Mathematics, Moscow State University, Vorob'evy gory, Moscow, 119899 Russia*

Received May 13, 1997

Abstract—Exhumation velocity and cooling rates were calculated for eclogites from the megamelange zone near Mount Sulu-Tyube in the Kokchetav Massif, Kazakhstan. The calculations were based on the reconstruction of the thermodynamic parameters of eclogite metamorphism during decompression and on modeling of the diffusion-controlled homogenization of a garnet grain with unusual growth zoning. The garnet is distinguished for strong compositional discontinuities between its outermost rim and euhedral core. Paragenetic analysis indicates that a garnet rim of distinct composition has developed around a garnet porphyroblast with the transition from the epidote amphibolite to eclogite metamorphic facies. A notable feature of the garnet is that its early core did not participate in the reaction and, thus, retained its euhedral habit. Our calculations indicate that the sharp boundaries between the garnet growth zones could be preserved after the growth stage only if the average exhumation velocity of the rock and its cooling rate were very high: 62 mm/year and 318°C/m.y., respectively.

INTRODUCTION

The Kokchetav median mass is a unique geological structure, whose interiors contain recently discovered economic reserves of diamond. Along with other high-pressure minerals, such as coesite, K-bearing pyroxene, aluminous rutile, and sphene, diamond was found as inclusions in some rock-forming minerals of the metamorphic rocks, which show very unusual textural and compositional features [1–4]. All of the metamorphic rocks compose a continuous megamelange zone [5]. Hence, the problem of the preservation of the high- and ultrahigh-pressure mineral assemblages and the mechanism of rock exhumation from depths that are much larger than the average crust thickness can be resolved only if the fullest information is invoked on the P–T–t evolution of various rock types within the tectonic zone.[1] In conjunction with this broader problem, we examined boudined eclogites from the foot of Mount Sulu-Tyube, where the silicate melange is mapped most clearly [5]. It was found that the garnet of the rocks possesses a very unusual growth zoning. Below, we will analyze the causes of this zoning and the conditions of its preservation at high temperatures and pressures. Our study resulted in direct estimates of the uplift velocity and cooling rate of the eclogites in the Kokchetav metamorphic complex.

[1] Notation: T—temperature, P—pressure, t—time. Mineral symbols: *Ab*—albite, *Alm*—almandine, *Amp*—amphibole, An_5—anorthite and its mole fraction in plagioclase, *Cpx*—clinopyroxene, *Ep*—epidote, *Czo*—clinozoisite, *Grt*—garnet, *Grs*—grossular, Jd_{29}—jadeite and its mole fraction in *Cpx*, *Omp*—omphacite, *Prp*—pyrope, *Sps*—spessartine. X_{Mg} = Mg/(Mg + Fe), X_{Ca} = Ca/(Ca + Mg + Fe).

OVERVIEW OF THE PETROGRAPHY AND MINERALOGY OF THE ECLOGITE

The major rock-forming minerals of the eclogite are garnet, omphacite (which contains up to 28% *Jd*), clinozoisite, quartz, and rutile. The rock is gneissose, with a porphyritic granoblastic texture. Retrograde effects in the eclogite resulted in kelyphytic rims of amphibole around garnet porphyroblasts and clinopyroxene (Jd_{2-6})–plagioclase (An_{13-17}) symplectite (often with amphibole) along the boundaries of omphacite grains.

The high-contrast back-scattered electron image of Fig. 1 [6] shows the clearly distinct core and rim of a garnet grain. The clear-cur outlines of the core accentuate the euhedral habit of the early (preeclogitic) garnet. Its growth zones display systematic variations in the composition of mineral inclusions that were entrapped during the prograde metamorphic stage. The garnet core contains coexisting clinozoisite, calcite, and plagioclase. More calcic (An_{26}) in the core, the plagioclase approaches albite (An_5) in the rim. The rim is dominated by pargasitic amphibole, clinozoisite (which is poorer in pistacite than the clinozoisite in the core), and quartz. All inclusions are situated closer to the inner part of the rim. The compositions of the minerals are presented in table. The analyses were obtained at the Laboratory of High-Resolution Analytical Techniques of Moscow State University.

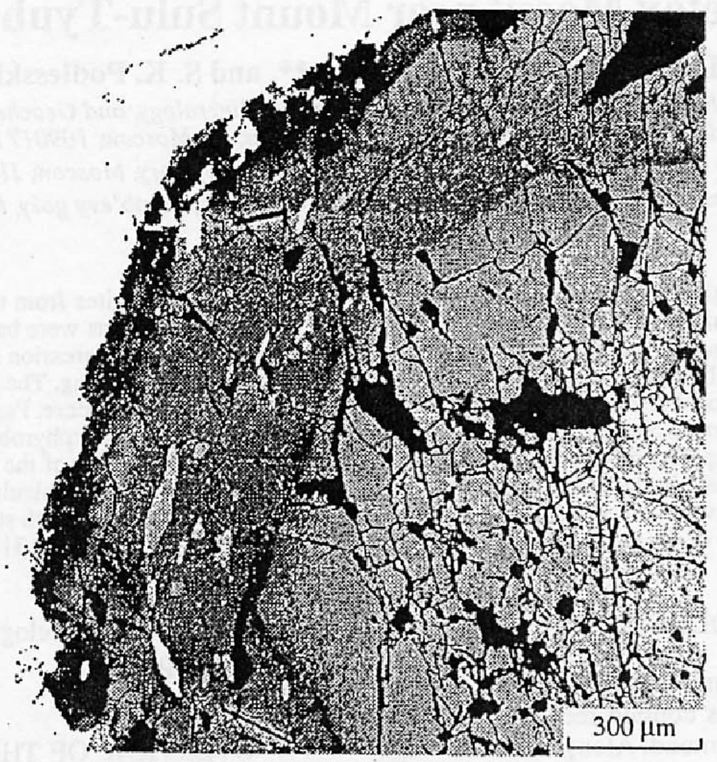

Fig. 1. Back-scattered electron image of a garnet porphyroblast. The boundary between the core and marginal zone is very sharp, and the core shows an euhedral habit.

GARNET CHEMISTRY AND CAUSES OF ITS ZONING

The overall heterogeneity of the garnet, pronounced in back-scattered electron images (Fig. 1), was refined with microprobe profiles. It was determined that the high contrast between the core and outer rim is determined by a stepwise increase in the content of Ca and an analogous decrease in the content of Fe (Fig. 2, table), whereas the compositional variations within the core are much smoother.

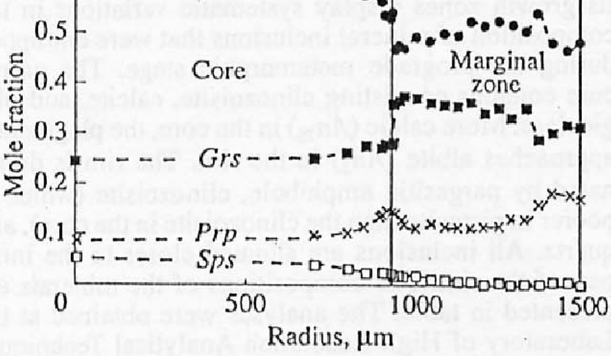

Fig. 2. Microprobe profile across the garnet grain portrayed in Fig. 1. The boundary between the core and outer rim is marked by a rapid increase in the content of grossular (*Grs*) and decrease in the almandine concentration (*Alm*); neither pyrope (*Prp*) nor spessartine (*Sps*) contents show significant variations in the high-gradient zone. Growth zones differ in the composition of mineral inclusions.

No analogous compositional variations have ever been determined in garnet from eclogites. The causes of this phenomenon can be elucidated by means of chemographic paragenetic analysis of the mineral relationships in the rock.

From the composition of mineral inclusions in the garnet, it is clear that the protolith of the eclogite was epidote–garnet amphibolite. Relics of its mineral assemblages are the euhedral garnet cores of large garnet porphyroblasts, clinozoisite, amphibole, and quartz inclusions in the rim. The inclusions (clinozoisite and plagioclase) in the garnet core were isolated by the idioblast itself and can most probably be attributed to the assemblage of the epidote amphibolite. The AC[FM] triangular plot in Fig. 3 displays the actual compositions of the minerals of the epidote amphibolite and those of the eclogitic assemblage (the garnet in the rim and omphacite). As can be seen from the plot, the compositions from the garnet core lie to the right of the amphibole field, whereas the eclogitic garnet (from the rim) is plotted to the left of it. At this relative position of the minerals, tie-lines connecting the equilibrium compositions of the eclogitic garnet and omphacite are intersected only with amphibole–clinozoisite

Microprobe analyses and cation proportions of minerals in the Sulu-Tyube eclogite

Component	Garnet core	Transition high-gradient zone in garnet (analyses are spaced 10 μm apart)							Garnet rim		
	Grt(1) core	*Grt*(1–2)							*Grt*(2)		
SiO_2	37.39	37.32	37.34	37.32	37.83	37.95	38.00	37.58	37.63	38.14	37.75
TiO_2	0.14	0.04	0.00	0.00	0.00	0.15	0.07	0.11	0.02	0.00	0.05
Al_2O_3	20.94	21.68	21.29	21.35	21.43	21.43	21.62	21.40	21.57	21.79	21.69
FeO	28.15	26.58	26.40	26.13	25.97	22.80	22.84	23.31	23.68	23.80	23.77
MnO	2.45	1.07	1.03	1.01	0.78	0.82	0.89	0.65	0.78	0.46	0.42
MgO	2.21	3.53	3.63	3.88	3.76	3.62	3.31	3.06	2.78	2.73	4.84
CaO	8.72	9.71	10.09	10.03	10.20	13.00	13.26	13.72	13.51	12.85	11.10
Na_2O	0.00	0.08	0.18	0.27	0.00	0.21	0.00	0.15	0.00	0.17	0.38
K_2O	0.00	0.00	0.05	0.01	0.03	0.03	0.00	0.02	0.03	0.06	0.00
Total	100.00	100.00	100.00	100.00	100.00	100.00	100.00	100.00	100.00	100.00	100.00
Si	2.98	2.94	2.94	2.94	2.97	2.96	2.97	2.95	2.95	2.99	2.94
Al	1.97	2.02	1.98	1.98	1.98	1.97	1.99	1.98	2.00	2.01	1.99
Ti	0.01	0.00	0.00	0.00	0.00	0.01	0.00	0.01	0.00	0.00	0.00
Fe^{3+}	0.04	0.04	0.08	0.08	0.04	0.06	0.03	0.07	0.05	0.00	0.07
Fe^{2+}	1.83	1.71	1.66	1.64	1.66	1.43	1.46	1.46	1.51	1.56	1.48
Mn	0.17	0.07	0.07	0.07	0.05	0.05	0.06	0.04	0.05	0.03	0.03
Mg	0.26	0.41	0.43	0.46	0.44	0.42	0.39	0.36	0.33	0.32	0.56
Ca	0.74	0.82	0.85	0.85	0.86	1.09	1.11	1.15	1.14	1.08	0.93
Na	0.00	0.01	0.03	0.04	0.00	0.03	0.00	0.02	0.00	0.03	0.06
K	0.00	0.00	0.00	0.00	0.00	0.00	0.00	0.00	0.00	0.01	0.00
Total	8.01	8.03	8.04	8.05	8.02	8.03	8.01	8.04	8.02	8.02	8.06
X_{Mg}	0.12	0.19	0.20	0.21	0.20	0.22	0.20	0.19	0.17	0.17	0.27
X_{Ca}	0.25	0.27	0.28	0.28	0.28	0.36	0.37	0.38	0.38	0.36	0.31

Component	Eclogite mineral assemblage			Retrograde minerals				Inclusions in garnet			
	Grt(2) rim with *Omp*	*Omp* rim with *Grt*	*Omp* core	*Cpx*	*Pl*	*Amp*	*Pl*	*Ep*(1)	*Pl*(1)	*Amp*(2)	*Czo*(2)
				symplectite		symplectite					
SiO_2	38.52	54.46	54.46	53.80	64.25	46.17	65.48	39.14	60.87	44.36	40.00
TiO_2	0.07	0.18	0.18	0.13	0.10	0.16	0.00	0.00	0.00	0.35	0.11
Al_2O_3	21.75	7.33	7.33	1.73	21.87	12.57	21.25	28.28	24.20	16.01	32.48
FeO	22.66	5.04	5.04	5.84	0.14	13.39	0.33	8.36	0.61	13.98	2.36
MnO	0.11	0.00	0.00	0.00	0.03	0.13	0.02	0.05	0.11	0.09	0.00
MgO	5.25	10.90	10.90	14.07	0.28	13.08	0.07	0.02	0.00	10.72	0.09
CaO	11.61	18.25	18.25	23.21	3.58	11.22	2.26	24.16	5.56	10.49	24.84
Na_2O	0.04	3.85	3.85	1.18	9.75	3.03	10.55	0.00	8.59	3.45	0.05
K_2O	0.00	0.00	0.00	0.05	0.00	0.25	0.04	0.00	0.03	0.55	0.08
Total	100.00	100.00	100.00	100.00	100.00	100.00	100.00	100.00	99.97	100.00	100.00
Si	2.98	1.97	1.97	1.97	2.84	6.53	2.88	2.97	2.71	6.32	2.99
Al	1.98	0.31	0.31	0.07	1.14	2.10	1.10	2.53	1.27	2.69	2.86
Ti	0.00	0.00	0.00	0.00	0.00	0.02	0.00	0.00	0.00	0.04	0.01
Fe^{3+}	0.03	0.01	0.03	0.06	–	0.53	–	0.53	–	0.34	0.15
Fe^{2+}	1.43	0.14	0.13	0.12	0.01	1.05	0.01	–	0.02	1.33	–
Mn	0.01	0.00	0.00	0.00	0.00	0.02	0.00	0.00	0.00	0.01	0.00
Mg	0.61	0.59	0.59	0.77	0.02	2.76	0.00	0.00	0.00	2.28	0.01
Ca	0.96	0.71	0.71	0.91	0.17	1.70	0.11	1.96	0.27	1.60	1.99
Na	0.01	0.27	0.27	0.08	0.83	0.83	0.90	0.00	0.74	0.95	0.01
K	0.00	0.00	0.00	0.00	0.00	0.05	0.00	0.00	0.00	0.10	0.01
Total	8.01	4.00	4.00	4.00	5.01	15.58	5.02	8.00	5.02	15.66	8.01
X_{Mg}	0.30	0.81	0.82	0.87	–	0.64	–	–	–	0.58	–
X_{Ca}	0.32		–	–	0.17	–	0.11	–	0.26	–	–
X_{Jd}	–	0.27	0.27	0.02	–	–	–	–	–	–	–

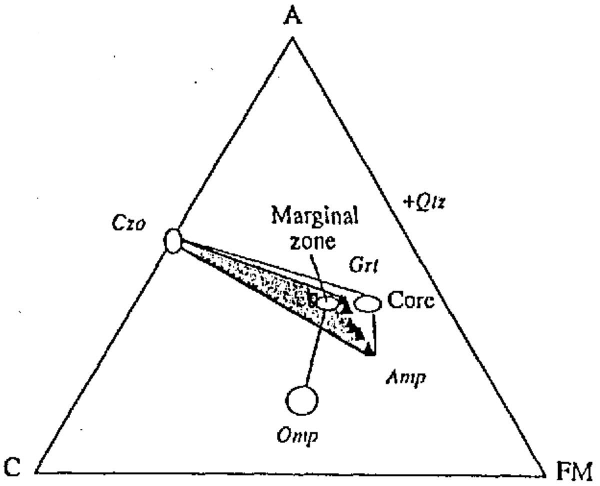

Fig. 3. Triangular ACFM [Al : Ca : (Fe,Mg)] plot showing the composition and assemblages of the main high-pressure minerals (omphacite and garnet) from the rim and analogous features of the epidote-amphibolite minerals (clinozoisite, amphibole, and garnet in the porphyroblast core). The tie-lines connecting *Omp* and *Grt* in the rim intersect only *Czo–Amp* tie-lines (shaded area), a fact indicating that eclogitization occurred during the prograde stage according to the reaction *Czo* + *Amp* ⟶ *Grt* rim) + *Omp* + H_2O. The early garnet in the core did not take part in the reaction.

tie-lines. This means [7] that the high-pressure garnet and omphacite developed exceptionally at the sacrifice of decomposing clinozoisite–amphibole assemblage. To state it otherwise, the eclogitization of the epidote–garnet amphibolite can be expressed as the dehydration reaction

$$\underset{\text{epidote amphibolite}}{\text{amphibole + clinozoisite}} \longrightarrow \underset{\text{eclogite}}{\text{(Ca–Mg)-garnet + omphacite} + H_2O}. \quad (1)$$

Reaction (1) not only describes the transition between the epidote amphibolite and eclogite facies but also explains the origin of the high-gradient interval between the core and rim of the garnet. Since the euhedral Fe–Mn garnet did not participate in this reaction, the new Ca–Mg garnet overgrew the preexisting crystal, which did not change either its composition or the original euhedral habit. This suggests that the transition from the core to the periphery occurred very rapidly. The corresponding high-gradient interval within the garnet grain, which was detected in microprobe profiles, resulted from the partial homogenization of the garnet during the retrograde stage. Let us quantify this process by using the following model.

SIMULATION OF DIFFUSION IN GARNET

Volume diffusion in a garnet grain with a growth zoning can be described with a model for diffusion in a sphere [7–10]. The general equation of diffusion of component *i* is

$$\frac{\partial C}{\partial t} = D(t)\left(\frac{\partial^2 C}{\partial r^2} + \frac{2}{r}\frac{\partial C}{\partial r}\right); \quad (0 \le r \le a), \qquad (2)$$

where a is the radius of the sphere, $C(r, t)$ is the desired dependence between the concentration of component *i* at a distance r from the center of the sphere (garnet crystal) and time t, an $D(t)$ is the diffusion coefficient of component *i* expressed as a function of time.

As can be seen in the profile across the garnet grain (Fig. 2), the rapid transition between the core and rim is pronounced most strongly in the concentration variations of Ca and Fe. Experimental data [11] indicate that the diffusion coefficient of Ca in garnet is more than one order of magnitude lower than the analogous coefficients for Fe, Mg, and Mn [12]. According to the theory of multicomponent diffusion [13, 14], component transport across a high-gradient zone in garnet is primarily controlled in this case by the diffusion of Ca, and, hence, our model can be described when (2) is resolved for the unknown function of Ca concentration.

A theoretical solution of (2) requires formulating the boundary and initial conditions.

Boundary conditions. Our concern is only the diffusion process within the high-gradient zone. In this case, the rim of the garnet grain prevents the introduction of isomorphous components into the zone from outside (for example, from the fluid and neighboring minerals). Thus, we will assume that the system is closed. The condition of the absence of mass exchange with the environment can be expressed as

$$\left.\frac{\partial C}{\partial r}\right|_{r=0} = 0, \quad \left.\frac{\partial C}{\partial r}\right|_{r=a} = 0. \qquad (3)$$

Initial conditions. The choice of initial conditions presents the main challenge in solving problems of this type. In fact, the principal task is to reconstruct the original growth zoning of the mineral. In practice, it is very difficult to determine whether a given zoning pattern was originally caused by growth or underwent partial homogenization. However, the problem will be significantly simplified in the case of garnet grains with compositional discontinuities between the cores and margins if the discontinuities are assumed to reflect the original transition between the core and rim. Since this configuration of a profile is close to that observed in our garnet, the error in the choice of the boundary conditions should not be large (compare with [10, 13]). The corresponding initial conditions will be

$$\begin{aligned} C(0 \le r < h, t = 0) &= C_1, \\ C(h \le r \le a, t = 0) &= C_2, \end{aligned} \qquad (4)$$

where h is the distance from the grain center to the core–rim transition zone, and C_1 and C_2 are the corresponding contents of Ca in the immediate neighborhood of the high-gradient zone (Fig. 2).

An expression of this type for the initial conditions implies that both the core and the rim are homogeneous. Of course, this is a very rough approximation, but in this case, our main concern is the preservation conditions of the high compositional gradient within a narrow (about 15 μm) zone of the garnet grain. If the diffusion process did not expand beyond this zone, this process was virtually independent of the concentration at a large distance (for example, at 200 μm) from the transition zone.

Solution. To simplify the search for the system solution, let us proceed to dimensionless radius and time variables. The dimensionless time is understood as

$$t' = \int_0^t \frac{D(\tau)}{a^2} d\tau, \qquad (5)$$

where τ is the integration parameter, and $D(\tau)$ is the diffusion coefficient. The dimensionless radius will be

$$r' = r/a.$$

In this manner, we get rid of the $D(t)$ coefficient in equation (2) and obtain a value for the radius, which can range between 0 and 1.

The overall diffusion equation for an isolated sphere as a function of these variables was presented elsewhere [9, 13], and, hence, we will list here only its partial solution that complies with new initial condition (4)

$$C(r', t') = b^3 C_1 + (1 - b^3) C_2 + \frac{2}{r'} \sum_{n=1}^{\infty} \exp(-\beta_n^2 t') \frac{\sin(\beta_n r')}{\sin^2 \beta_n} A_n, \qquad (6)$$

where

$$A_n = \frac{1}{\beta_n^2}((C_2 - C_1)(b\beta_n \cos b\beta_n - \sin b\beta_n) - C_2(\beta_n \cos \beta_n - \sin \beta_n)),$$

and β_n are the roots of the equation $\beta_n \cot(\beta_n) = 1$, $b = h/a$.

We calculated lines of the sequential relaxation of the high-gradient zone from equation (6) for $t' = 10^{-5}$, 10^{-4}, and 10^{-3} (Fig. 4). As can be seen from this plot, the profile observed in the garnet is best fit by the line for $t' = t'_s = 10^{-5}$.

This value of the dimensionless time should be regarded as a quantitative parameter of garnet homogenization. With the use of equation (4), this quantity can be employed as a sensitive indicator of the thermal and baric rates of eclogite evolution [10, 13] if the *P–T* parameters of metamorphism are known.

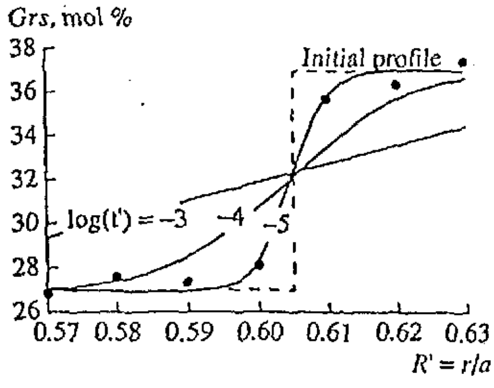

Fig. 4. Homogenization trajectories calculated [by equation (6)] for the high-gradient zone in the garnet as a function of the dimensionless time parameter (t'), grossular mole fraction in the garnet, and dimensionless radius R' (a = 1500 μm). The initial profile corresponds to the compositional discontinuity between the core and rim of the garnet at $t' = 0$. Microprobe profile is best fitted by a calculated trajectory with $t' = 10^{-5}$.

P–T PARAMETERS OF METAMORPHISM

Eclogite stage. The peak temperature of eclogite metamorphism was determined on the basis of the compositions of coexisting garnet and omphacite, which were analyzed at a distance of ~3 μm from the physical contact of the grains. The temperature was estimated by the garnet–clinopyroxene geothermometer [15] (see [16] for details) at 680 ± 50°C. It is worth noting that the origin of the minerals during the eclogite metamorphic stage was confirmed by microprobe profiles across the contact zones, which contain no discernable traces of retrogression. The minimum pressure during the metamorphic climax was evaluated by the clinopyroxene–quartz–plagioclase geobarometer [17]. At a jadeite content in the clinopyroxene of 29 mol %, the pressure was estimated at 14 kbar, i.e., the equilibrium conditions of the eclogite were T = 680°C and $P \geq 14$ kbar. These values are consistent with the estimates obtained by Shatsky *et al.* [4].

Retrograde stage. It was noted above that retrograde metamorphism manifests itself in the eclogites in the form of continuous reactions of symplectite formation and the growth of kelyphytic amphibole. The clinopyroxene–plagioclase symplectite of this stage can be utilized as a geobarometer. At the same time, the kelyphyte rims are apparently reaction textures that develop after the garnet, and, thus, their margins cannot be used to estimate the temperature [16]. Neither can the temperature of the retrograde stage be determined by the coexisting garnet and omphacite, because they did not experience retrograde Fe and Mg redistribution. However, the high thermal relaxation rate of eclogite bodies in the melange zone (see, for example, [18]: a lens-shaped eclogite body 200 m thick should cool to the host-rock temperature for as little as ~317 years at $k \approx 10^{-6}$ m^2/s) enables the evaluation of the retrograde

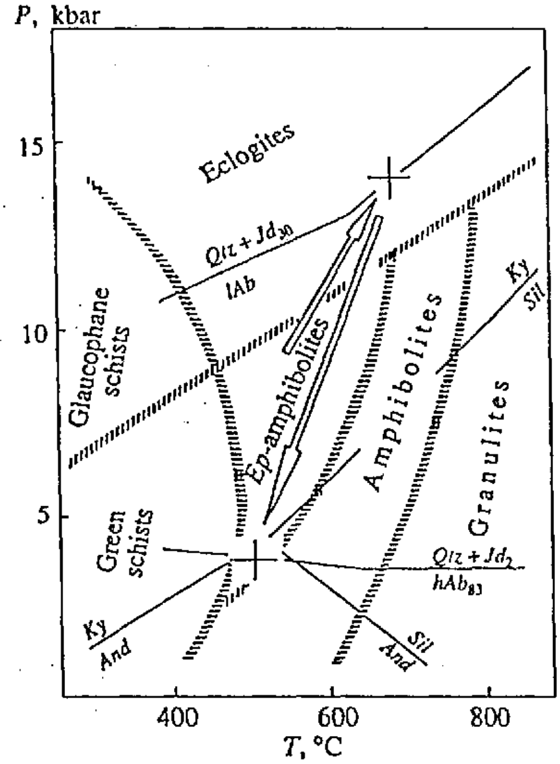

Fig. 5. Petrogenetic grid showing the *P–T* metamorphic trajectory of the Sulu-Tyube eclogite. The parameters of the main metamorphic stages were determined by geothermobarometry (see text). Metamorphic facies are portrayed in accordance with [18], the stability of aluminum silicate is shown after [21], and the albite = jadeite + quartz monovariant equilibrium is given according to [17] (estimate based on the composition of the coexisting clinopyroxene and plagioclase; superscript indexes denote the mole fractions of respective end-members).

metamorphic temperature by the host rocks [19, 20]. In this case, we used the value of 500°C for the host garnet–andalusite–biotite and biotite–muscovite gneisses and schists [5]. At this temperature, the calculated pressure value [17] was 4 kbar. It should be noted that our estimates, obtained using clinopyroxene with 2 mol % jadeite and coexisting plagioclase An_{17}, is fully consistent with the stability of andalusite in the host gneisses [21].

P–T path. A generalized evolution pattern of the physical conditions of metamorphism is portrayed in the *P–T* plot of Fig. 5 as prograde and retrograde trajectories. The prograde trajectory reflects the transition from the epidote amphibolite to eclogite facies. At the boundary between the facies, the mineral assemblages were fully transformed, and a high-gradient zone appeared between the core and rim of the garnet (Fig. 3). The peak of eclogite metamorphism occurred at $T = 680°C$ and $P \geq 14$ kbar. The mineral assemblages provide evidence of a vertical displacement of the rocks for approximately 35 km, which is a significant value for crystalline rocks. A considerable part of this uplift occurred under epidote amphibolite-facies conditions, as the temperature and pressure decreased to 500°C and 4 kbar. The high-pressure paragenesis, fragments of the preeclogitic assemblage, and the high-gradient zoning in the garnet were almost fully preserved. In this connection, it is expedient to examine the dynamics of the temperature and pressure changes during the exhumation of the rocks.

UPLIFT VELOCITIES AND COOLING RATES OF ECLOGITE

Relation (5) makes it possible to estimate the *P–T–*t trajectories in terms of dimensionless time (t') and compare them with the homogenization degree of individual garnet grains [9, 10, 13, 22]. According to the *P–T* path (Fig. 5), the uplift magnitude of the rocks was 35 km ($\Delta P = 10$ kbar). We now can determine the time (t) of the process for any specified value of uplift velocity. For example, at an uplift velocity of 1 mm/year, the rocks would have been exhumed from a depth of 35 km for 35 m.y. Along with time, relation (5) includes the diffusion coefficient of Ca and the radius of the garnet grain. The dependence of a diffusion coefficient on temperature is expressed as the Arrhenius equation

$$D(t) = D_0 \exp\left(\frac{-E_a}{RT(t)}\right),$$

where D_0 is the preexponential factor, E_a is the activation energy of Ca diffusion, R is the universal gas constant, and $T(t)$ is the temperature expressed as a function of time. The parameters $D_0 = 7.2 \times 10^{-16}$ m²/s and $E_a = 15$ kJ/mol were compiled from [11], which is now the only experimental study devoted to the self-diffusion of Ca in garnet.

The restriction of the process to a local zone distant from the margin of the grain (Fig. 4) permitted us to use in relation (5) the radius of the outer boundary of the high-gradient zone (1000 μm) instead of the radius of the whole crystal. Our calculation results were plotted in a diagram that exhibits the relationships between the dimensionless time and the uplift velocity of the rock (Fig. 6). Knowing the homogenization degree of the garnet ($t' = 10^{-5}$), we estimated, using the plot, the velocity of eclogite uplift at 6.2 cm/year. This value demonstrates that the eclogite was exhumed from the lower crust and covered a vertical distance of 35 km for the relatively brief period of time of merely 0.6 m.y. The corresponding cooling rate of the rock was 319°C/m.y. It is pertinent to note that this first determination of the velocity of eclogite exhumation in the Kokchetav Massif significantly exceeds all preexisting estimates of rock exhumation velocities obtained for high-pressure complexes (see Table 3 in [13]).

DISCUSSION

The traditional technique used to determine the uplift velocities and cooling rates of high-pressure rocks (for example, [23]) are based on geothermobarometric data coupled with geochronological dates of the principal metamorphic stages. The uplift velocity (cooling rate) is calculated as the ratio of the pressure (temperature) difference to the difference in the radiological age. However, this approach requires more strict control over the radiological data and interpretation of the radiological age of eclogite metamorphism (see Table 3 in [13]). In order to clarify the aforesaid, let us consider a Sm–Nd mineral isochron (on garnet, clinopyroxene, and zoisite) for the Sulu-Tyube eclogite [24]. The isochron corresponds to an age of 465 ± 32 Ma. However, even the authors themselves admit that this values does not correspond to any definite geologic event. The results of our study demonstrate the necessity of a close preliminary examination of the garnet. In fact, the garnet consists of two independent systems (growth zones), each of which shows its own equilibrium distribution of elements. The inner zone (grain core) crystallized during epidote amphibolite metamorphism, whereas the outer zone (rim) was produced during eclogite metamorphism. Considering the similarity of the Sm and Nd diffusion coefficients in garnet [25] with analogous values for Ca, Fe, and Mg [11, 12], it is logical to suggest that, by analogy with the major isomorphous components, the Sm and Nd distribution in the garnet varies in its distinct growth zones. In other words, the Sm–Nd ratios in the garnet core and rim should correspond to the age of the epidote amphibolite and eclogite metamorphism, respectively. When a geochronologic study is conducted without taking into account the zoning pattern of the garnet, it yields overestimated age values. The possible errors can be roughly quantified on the basis of the study [26], in which it was demonstrated that the Sm–Nd age of the metamorphic peak shows a spread of 16 m.y. when determined on the core and margin of the same garnet grain. Hence, in search for realistic age values of metamorphic events with the use of zoned garnet crystals, it is advisable to separate distinct fractions (growth zones) of the garnet.

As was mentioned above, the Sm–Nd age of the Sulu-Tyube eclogite was estimated at 465 ± 32 Ma [27]. However, the actual age of the peak of eclogite metamorphism could be somewhat younger, because such estimates should be carried out only on the outermost (apparently the youngest) crystal zones. On the one hand, this will increase the difference between the metamorphic age of the Sulu-Tyube eclogite and the surmised age of the ultrahigh-pressure metamorphism (~530 Ma) obtained for rocks from the Kumdy-kul' area [27] and, on the other, make the former age closer to the emplacement time of the main phase of the Zerenda granitoid pluton (444 ± 9 Ma [28]). This closeness is very important for explaining the exhumation of the high-pressure rocks under the effect of gravitation-controlled ordering and crustal diapirism [29]. The results of numerical simulation of this process indicate that fragments of very dense eclogites can ascend, under the effect of convection, through rocks of lower density and viscosity (for example, two-mica schists) with velocities close to those calculated for the Sulu-Tyube eclogite (62 mm/year).

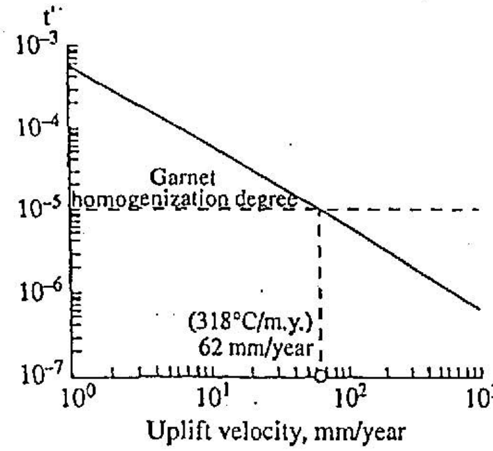

Fig. 6. Dependence of the homogenization degree of garnet (t') on the uplift velocity of the eclogite. Values of t' were calculated by equation (5) for the retrograde branch of the metamorphic trajectory (Fig. 5) and a garnet grain 1000 μm in diameter (see text). The uplift velocity (and cooling rate) of the eclogite were calculated from the known homogenization degree of the garnet ($t' = 10^{-5}$).

At the same time, a consensus was reached by many researchers of the megamelange zone of the Kokchetav Massif that the exhumation of the high- and ultrahigh-pressure rocks from significant depths could be caused by the backward flow of material in the accretionary wedge above a subducted plate [30]. The results of a geodynamic modeling of the process indicate that the velocity of the backward flow can be as high as the subduction velocity [31] or even exceed it [32]. The high-density Sulu-Tyube eclogite was exhumed with precisely this velocity of 6.2 cm/year, a fact that provides additional arguments for this geotectonic scenario. However, the information available so far is insufficient to choose between the two geotectonic scenarios.

The estimates obtained on the exhumation velocity and cooling rate of the eclogite need some comments. The value of $t'_s = 10^{-5}$ that was used in determining the uplift velocity (Fig. 4) corresponds to the maximum homogenization degree of the garnet. However, the original profile of the garnet could differ from that chosen in our case and, in the limiting case, even coincide with the microprobe profile (Fig. 4). For such a garnet that was not homogenized, $t' = t'_s = 0$. This means that t'_s can only decrease (see [13] for detail). To state it otherwise, possible corrections of the original profile morphology can result only in an increase of the calculated uplift velocity and cooling rate of the eclogite (Fig. 6). Nevertheless, the uncertainty interval t_s^i = [0; 10^{-5}] is so narrow (compare with [13]) that it justifies the accuracy of the reconstructed initial conditions.

It is also worth noting that, in determining the uplift velocity of the eclogite (Fig. 6), we assumed that the initial *P–T* parameters corresponded to the peak parameters of eclogite metamorphism. However, the high-gradient interval that was used to determine the uplift dynamics originated earlier, during the prograde metamorphic stage. Hence, strictly speaking, the calculation of t' should be begun with determining the *P–T* conditions under which the epidote–garnet amphibolite was transformed into eclogite according to reaction (1), and this would definitely increase the duration of the process modeled. The required thermodynamic data (for example, the water activity) are not available now, and the precise position of dehydration reaction (1) in a *P–T* plot cannot be determined (the corresponding boundary line between metamorphic facies in Fig. 5 is quite schematic). This disables us to introduce necessary corrections into the initial conditions of the simulated process. Nevertheless, it is fairly clear that the addition of a high-temperature prograde episode to the postgrowth history of the garnet will result in a further increase of the calculated uplift velocity and cooling rate.

It follows from analysis of the uncertainties in the simulation of the diffusion process in garnet that further refinement of our results will lead only to an increase in the calculated uplift velocity and cooling rate of the eclogite. This provides additional evidence of the unique nature of the Kokchetav Massif not only in the mineralogical but also in the geodynamic sense.

CONCLUSIONS

(1) The cores of garnet porphyroblasts in the Sulu-Tyube eclogite consist of euhedral crystals. The boundaries between the cores and marginal zones of the garnet are marked by a very strong increase in the content of grossular at decreasing content of almandine.

(2) We determined, using paragenetic analysis, that the rim of the garnet resulted from the dehydration reaction epidote + amphibole ⟶ garnet + omphacite + H_2O, which describes the transition between the epidote amphibolite and eclogite metamorphic facies. The early garnet did not participate in this reaction and retained its euhedral habit as the younger garnet grew during eclogitization.

(3) The preservation conditions of the high-gradient zone of the garnet were determined by means of geothermobarometry of the rocks and simulation of the homogenization process in the garnet.

(4) In tackling the diffusion problem, we managed to reach the most precise description of the process by obtaining the optimum set of initial conditions. Our modeling results demonstrate that the decompression of the eclogite from 680°C and 14 kbar to 500°C and 4 kbar occurred at very high uplift velocities and cooling rates, up to 6.2 cm/year and 319°C/m.y., respectively.

ACKNOWLEDGMENTS

The authors thank L.L. Perchuk and I.D. Ryabchikov for critical comments expressed during the preparation of the manuscript. The samples were provided by courtesy of A.A. Marakushev. We appreciate the participation of P. Philippot in the discussion of our results. The microprobe analyses were made with the help of N.N. Korotaeva and E.V. Guseva. This study was supported by the Russian Foundation for Basic Research, project nos. 97-05-64418 and 96-05-64396.

REFERENCES

1. Perchuk, L.L., Yapaskurt, V.O., and Okai, A., Comparative Petrology of Diamond-bearing Metamorphic Complexes, *Petrologiya*, 1995, vol. 3, pp. 267–309.
2. Sobolev, N.V. and Shatsky, V.S., Diamond Inclusions in Garnets from Metamorphic Rocks: A New Environment for Diamond Formation, *Nature*, 1990, vol. 343, pp. 742–746.
3. Shukolyukov, Yu.A., Pleshakov, A.M., and Lavrova, L.D., Uniquely High Content of $^3He/^4He$ in Diamonds from the Metamorphic Rocks of the Kokchetav Massif, Kazakhstan, *Petrologiya*, 1993, vol. 1, pp. 110–119.
4. Shatskii, V.S., Sobolev, N.V., and Gil'bert, A.E., Eclogites of the Kokchetav Massif, in *Eklogity i glaukofanovye slantsy v skladchatykh oblastyakh* (Eclogites and Glaucophane Schists in Fold Regions), Novosibirsk: Nauka, 1989, pp. 54–82.
5. Dobrzhinetskaya, L.F., Braun, T.V., Sheshkel, G.G., and Podkuiko, Yu.A., Geology and Structure of Diamond-bearing Rocks of the Kokchetav Massif (Kazakhstan), *Tectonophysics*, 1994, vol. 223, pp. 293–313.
6. Perchuk, A.L. and Varlamov, D.V., A New Type of Prograde Garnet Heterogeneity: An Example from the Eclogite of the Great Caucasus, *Geokhimiya*, 1995, vol. 9, pp. 1296–1310.
7. Korikovskii, S.P., *Fatsii metamorfizma metapelitov* (Metamorphic Facies of Metapelites), Moscow: Nauka, 1979.
8. Muncill, G.E. and Chamberlain, C.P., Crustal Cooling Rates Inferred from Homogenization of Metamorphic Garnets, *Earth Planet. Sci. Lett.*, 1988, vol. 87, pp. 390–396.
9. Jiang, J. and Lasaga, A.C., The Effect of Post-Growth Thermal Events on the Growth-Zoned Garnet: Implications for Metamorphic *P–T* History Calculations, *Contrib. Mineral. Petrol.*, 1992, vol. 105, p. 454.
10. Perchuk, A.L. and Philippot, P., Rapid Cooling and Exhumation of Eclogitic Rocks from the Great Caucasus, Russia, *J. Metamorph. Geol.*, 1997, vol. 15, pp. 299–310.
11. Schwandt, C.S., Cygan, R.T., and Westrich, H.R., Ca Self-Diffusion in Grossular Garnet, *Am. Mineral.*, 1996, vol. 81, p. 448.

12. Chakraborty, S. and Ganguly, J., Cation Diffusion in Aluminosilicate Garnets: Experimental Determination in Spessartine–Almandine Diffusion Couples, Evaluation of Effective Binary Diffusion Coefficients, and Applications, *Contrib. Mineral. Petrol.*, 1992, vol. 111, pp. 74–86.

13. Perchuk, A.L., Gerasimov, V.Yu., and Philippot, P., Theoretical Modeling of Eclogite Uplift, *Petrologiya*, 1996, vol. 4, pp. 518–532.

14. Chakraborty, S. and Ganguly, J., Compositional Zoning and Cation Diffusion in Garnets, *Advances in Physical Geochemistry*, 1991, vol. 8, pp. 121–175.

15. Krogh, E.G., The Garnet–Clinopyroxene Fe–Mg Thermometer—Reinterpretation of Existing Experimental Data, *Contrib. Mineral. Petrol.*, 1988, vol. 99, pp. 44–48.

16. Perchuk, A.L. and Gerasimov, V.Yu., Main Features of the Metamorphic Evolution of Eclogites from the Bol'shaya Laba Basin, Northern Caucasus, *Izv. Ross. Akad. Nauk, Ser. Geol.*, 1992, vol. 3, pp. 40–52.

17. Perchuk, A.L., A New Variant of the Omphacite–Albite–Quartz Geobarometer Accounting for the Structural States of Omphacite and Albite, *Dokl. Akad. Nauk SSSR*, 1992, vol. 324, pp. 1286–1289.

18. Spear, F.S., *Metamorphic Phase Equilibria and Pressure–Temperature–Time Paths*, Washington, DC: Min. Soc. Am., 1993.

19. Perchuk, A.L., Metamorphism of Kyanite Eclogite from the Krasnaya Skala Area, Front Range of the Great Caucasus, *Petrologiya*, 1993, vol. 1, pp. 98–109.

20. Dunn, S.R. and Medaris, L.G., Jr., Retrograded Eclogites in the Western Gneiss Region, Norway, and Thermal Evolution of a Portion of Scandinavian Caledonides, *Lithos*, 1989, vol. 22, pp. 229–245.

21. Salje, E., Heat Capacities and Entropies of Andalusite and Sillimanite: Influence of Fibrolitization on the Phase Diagram of the Al_2SiO_5 Polymorphs, *Am. Mineral.*, 1986, vol. 71, pp. 1366–1371.

22. Perchuk, A.L. and Philippot, P., Rapid Cooling of Eclogites Deduced from Diffusion Modelling of Growth-Zoned Garnets, *Terra Nova*, 1995, vol. 7, p. 42.

23. Steltenpohl, M.G., Cymerman, Z., Krogh, E.J., and Kunk, M.J., Exhumation of Continental Basement during Variscan Lithospheric Delimitation and Gravitation Collapse, Sudety Mountains, Poland, *Geology*, 1993, vol. 21, pp. 1111–1114.

24. Shatskii, V.S., Jagoutz, E., Koz'menko, O.A., *et al.*, Age and Origin of the Eclogites of the Kokchetav Massif, Northern Kazakhstan, *Geol. Geofiz.*, 1993, vol. 34, pp. 47–58.

25. Burton, K.W., Kohn, M.J., Cohen, A.S., and O'Nions, R.K., The Relative Diffusion of Pb, Nd, Sr and O in Garnet, *Earth Planet. Sci. Lett.*, 1995, vol. 133, pp. 199–211.

26. Getty, S.R., Selverstone, J., Wernicke, B.P., *et al.*, Sm–Nd Dating of Multiple Garnet Growth Events in an Arc–Continent Collision Zone, Northwestern U.S. Cordillera, *Contrib. Mineral. Petrol.*, 1993, vol. 115, pp. 45–57.

27. Claoue-Long, J.C., Sobolev, N.V., Shatskii, V.S., and Sobolev, A.V., Zircon Response to Diamond Pressure Metamorphism in the Kokchetav Massif, USSR, *Geology*, 1991, vol. 19, p. 710.

28. Shatagin, K.N., *J. Conf. Abstr.*, 1996, vol. 1, no. 1, p. 559.

29. Perchuk, L.L., Podladchikov, Yu.Yu., and Polyakov, A.N., *P–T* Paths and Geodynamic Modelling of Some Metamorphic Processes, *J. Metamorph. Geol.*, 1992, vol. 10, pp. 311–319.

30. Dobretsov, N.L., Shatskii, V.S., and Sobolev, N.V., Comparison of the Kokchetav and Dabie Shan Metamorphic Complexes: Coesite- and Diamond-bearing Rocks and UHP–HP Accretional–Collisional Events, *Int. Geol. Rev.*, 1995, vol. 37, pp. 636–656.

31. Cloos, M., Flow Melanges: Numerical Modelling and Geologic Constraints on Their Origin in the Fransiscan Subduction Complex, California, *Bull. Geol. Soc. Am.*, 1982, vol. 93, pp. 330–345.

32. Dobretsov, N.L. and Kirdyashkin, A.G., *Glubinnaya geodinamika* (Deep Geodynamics), Novosibirsk: Ob'ed. Inst. Geol. Geokhim. Mineral. Sib. Otd. Ross. Akad. Nauk, 1994.